DOI:10.1002/ejic.201300827

The Oxonitridoborate $Eu_5(BO_{2.51(7)}N_{0.49(7)})_4$ and the Mixed-Valent Borates $Sr_3Ln_2(BO_3)_4$ (Ln = Ho, Er)

Henning A. Höppe,*[a] Karolina Kazmierczak,[a] Christine Grumbt,[a] Lisa Schindler,[a] Inga Schellenberg,[b] and Rainer Pöttgen[b]

Keywords: Mössbauer spectroscopy / Structure elucidation / Borates / Lanthanides / Strontium / Optical properties

The crystal structures of the mixed borates $Sr_3Er_2(BO_3)_4$ [*Pnma*, no. 62, $Z = 4$, $a = 738.08(2)$, $b = 1588.94(4)$, $c = 867.81(2)$ pm, 683 reflections, 70 parameters, $R1 = 0.037$, $wR2 = 0.077$] and $Sr_3Ho_2(BO_3)_4$ [*Pnma*, no. 62, $Z = 4$, $a = 738.45(7)$, $b = 1591.55(12)$, $c = 871.03(9)$ pm, 691 reflections, 59 parameters, $R1 = 0.069$, $wR2 = 0.098$] and europium oxonitridoborate $Eu_5(BO_{2.51(7)}N_{0.49(7)})_4$ [*Pnma*, no. 62, $Z = 12$, $a = 2232.2(5)$, $b = 1603.1(3)$, $c = 879.59(18)$ pm, 2880 reflections, 313 parameters, $R1 = 0.027$, $wR2 = 0.059$] were solved from single-crystal X-ray diffraction data. $Eu_5(BO_{2.51(7)}N_{0.49(7)})_4$ adopts a threefold superstructure of the structure of $Sr_3Ln_2(BO_3)_4$ (Ln = Ho, Er). In both structure types, the different cations are situated on common sites with a pronounced preferential occupation but no complete ordering. These conclusions are based on the crystal structure refinement, ^{151}Eu Mössbauer spectroscopy and MAPLE (Madelung part of lattice energy) calculations. The proposed $Eu_5(BO_3)_4$ contains nitrogen and has a formula $Eu_5(BO_{2.51(7)}N_{0.49(7)})_4$ as confirmed by ^{151}Eu Mössbauer spectroscopy. The optical reflectance spectrum of $Eu_5(BO_{2.51(7)}N_{0.49(7)})_4$ is in accordance with the yellow colour of the compound.

Introduction

Like many silicates and phosphates, borates also provide possible host structures for emitters that form phosphors for various optical applications.[1] In the course of our systematic investigation of such host compounds, we identified the mixed alkaline earth–rare earth borates $Sr_3Ln_2(BO_3)_4$ (Ln = Ho, Er) as promising candidates for simultaneous doping with divalent and trivalent emitters, as a first structural study revealed an ordered arrangement of strontium and rare-earth ions, respectively, in these compounds.[2] Compounds with such a cation ordering are desirable for future codoped phosphors, which might be useful for white light-emitting diodes (LEDs)[3] or quantum cutting phosphors for the replacement of mercury plasma tubes by xenon plasma tubes.[4]

A formal substitution of Sr^{2+} by Eu^{2+} ions, which are of a similar size, and the use of Eu^{3+} as a trivalent pendent could lead to the mixed-valent compound $Eu_5(BO_3)_4$, which was postulated as early as 1980[5] but has not yet been crystallised or proven otherwise. This borate would be the first to contain both Eu^{2+} and Eu^{3+} ions simultaneously. To date, only the europium borates EuB_4O_7,[6] $Eu_3B_2O_6$,[7] $Eu_2B_2O_5$, EuB_2O_4[6,8] (containing divalent europium), Eu_3BO_6, $EuBO_3$ and EuB_3O_6 (containing trivalent europium)[9] could be characterised. If high-pressure phases are also considered, europium borate chemistry is extended to α-$Eu_2B_4O_9$,[10] which also contains trivalent europium.

During our investigations, it became obvious that $Eu_5(BO_3)_4$ contains significant amounts of nitrogen and has the overall formula $Eu_5(BO_{2.51(7)}N_{0.49(7)})_4$. Many pure lanthanide nitridoborates such as $Pr_3B_3N_6$,[11] $Ln_3B_2N_4$ (Ln = La–Nd), $La_5B_4N_9$[12] and $Eu_3[BN_2]_2$[13] and the oxonitridoborate $Sr_3[B_3O_3N_3]$[14] are also known, but to the best of our knowledge europium oxonitridoborate is not known.

In a recent contribution, we shed light on the optical properties of the polyphosphates $Ln(PO_3)_3$ (Ln = Y, Gd–Lu),[15,16] in which we found an unprecedented partial in situ reduction of trivalent europium to the divalent state; thus, a mixed-valent europium compound forms but in this case is only realised on a relatively low doping level.

Herein, we present the crystal structure determination of the first europium oxonitridoborate $Eu_5(BO_{2.51(7)}N_{0.49(7)})_4$ and a redetermination of the crystal structures of $Sr_3Ln_2(BO_3)_4$ (Ln = Ho, Er), including the crystal–chemical relationships between them. Moreover, we applied Mössbauer spectroscopy to clarify the valence state of europium and the optical reflection spectroscopy of $Eu_5(BO_{2.51(7)}N_{0.49(7)})_4$.

---

[a] Institut für Physik, Universität Augsburg,
Universitätsstraße 1, 86159 Augsburg, Germany
E-mail: henning@ak-hoeppe.de
www.ak-hoeppe.de
[b] Westfälische Wilhelms-Universität Münster, Institut für Anorganische und Analytische Chemie,
Corrensstraße 30, 48149 Münster, Germany

Supporting information for this article is available on the WWW under http://dx.doi.org/10.1002/ejic.201300827.

Results and Discussion

The Crystal Structures of $Sr_3Er_2(BO_3)_4$, $Sr_3Ho_2(BO_3)_4$ and $Eu_5(BO_{2.51(7)}N_{0.49(7)})_4$

The crystal structures of $Sr_3Er_2(BO_3)_4$ and $Sr_3Ho_2(BO_3)_4$ are isotypic. In contrast to the previously published description, both adopt the centrosymmetric space group *Pnma* (no. 62) instead of the non-centrosymmetric $Pna2_1$ (no. 33). The crystal structure of $Eu_5(BO_{2.51(7)}N_{0.49(7)})_4$ is closely related to these and will be described in the second part of this section.

Crystal Structure of $Sr_3Ln_2(BO_3)_4$ (Ln = Er, Ho)

The arrangement of the structural moieties is very similar to that in the Gd_5Si_4 structure type [*Pnma*, a = 748.23(18), b = 1473.8(4), c = 774.60(18) pm].[17] The Ln/Sr atoms formally replace the gadolinium atoms in the structure of Gd_5Si_4, whereas the borate anions adopt the silicon sites. Thus, slightly compressed edge-sharing cubes (sites Sr2/Er2 and Sr3/Er3) centred on the remaining site Sr1/Er1 are formed. These cubes form square sheets parallel to the *ab* plane stacked along *c* in an AB stacking order. Between this packing of cations, the noncondensed borate anions are situated (Figure 1).

Normally, the different charges and sizes of atoms enable their ordering and result in significantly different bond lengths to their respective coordinating atoms. The coordination environments of the metal atoms are shown in Figure 2. The cations are eight- (Sr1/Er1) and sevenfold (Sr2/Er3, Sr3/Er3) coordinated by oxygen atoms. The oxygen atoms of the Sr/Er coordination environments form more or less distorted bicapped trigonal prisms [site Sr1/Er1, Sr/Er–O 237.7(11)–254.0(17) pm], square antiprisms [site Sr2/Er2, 241.3(11)–281.5(8) pm] and pentagonal bipyramids [site Sr3/Er3, 241.8(15)–268.4(8) pm]. The given distances agree well with the sum of ionic radii of 235 (Er–O) and 256 pm (Sr–O)[18] and do not indicate a clear preference for a certain ion. Therefore, we refined the relative Sr/Er occupations of each site. Site 1 is preferentially occupied by Er [69.5(1)%], whereas sites 2 and 3 are mainly occupied by Sr [68.4(3) and 66.4(3)%]. These values did not change significantly when using the non-centrosymmetric space group $Pna2_1$, which provided the chance for a complete ordering of the cations.

The borate anions consist of boron triangularly coordinated by oxygen atoms. The B–O bond lengths vary in a very small range from 134.5(8) to 135.7(6) pm, in good agreement with the sum of ionic radii (B–O) of 137 pm.[18] The O–B–O angles range between 114(1) and 124(1)°. The

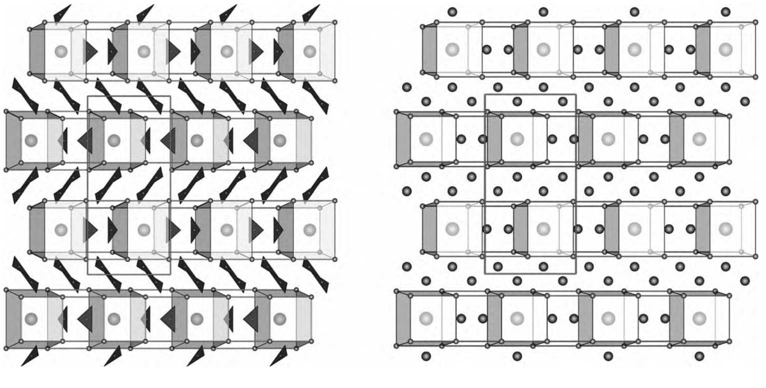

Figure 1. Representation of the crystal structures of $Sr_3Er_2(BO_3)_4$ and $Sr_3Ho_2(BO_3)_4$ compared with that of Gd_5Si_4; the Ln^{3+} ions are shown as large grey spheres (viewed approximately along [001]).

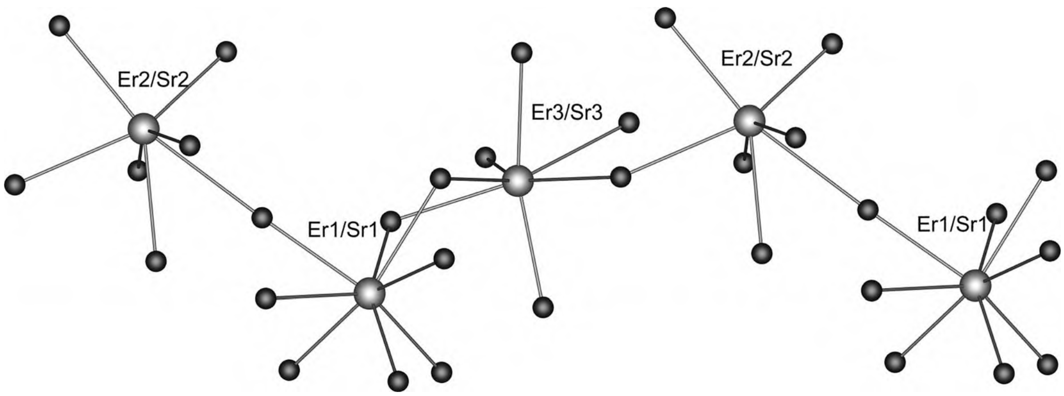

Figure 2. Coordination environments of the metal ions in $Sr_3Er_2(BO_3)_4$.

shortest B–B distances are between 469.10(1) and 473.41(1) pm.

In the previous structure determination (space group *Pna*2$_1$), a complete ordering of the cations was postulated. The distances in this structure model are very similar to those of our structure refinement. Therefore, we conclude that in the originally investigated single crystals only a partial ordering was present and the authors probably just missed the presence of inversion centres in their structure model.

Crystal Structure of $Eu_5(BO_{2.51(7)}N_{0.49(7)})_4$

$Eu_5(BO_{2.51(7)}N_{0.49(7)})_4$ crystallises in the space group *Pnma* as a threefold superstructure of the previously described crystal structure of $Sr_3Er_2(BO_3)_4$ along the *a* axis. Thus, the relationship between both structures can be classified as klassengleich of index 3 (Figure 3). The most prominent difference that causes the tripling of the unit cell is the changed orientation of the borate anion centred on B4 by 90° with respect to the *ab* plane (Figure 4). The aforementioned formal cubes are formed by sites Eu4–Eu9 and centred by Eu1, Eu2 and Eu3. The coordination distances of all europium ions lie within the usual range and are listed in Table 3. All distances and angles in the borate ions are within the typical ranges of 133.6(8)–141.1(9) pm and 114.2(6)–126.9(7)°, respectively.

As mentioned earlier, the composition of the europium oxonitridoborate is $Eu_5(BO_{2.51(7)}N_{0.49(7)})_4$ based on the refinement of single-crystal data. Accordingly, for the europium ions an average charge of +2.79(8) is yielded. The most reliable tool to confirm the direct ratio of the relative amounts of Eu^{2+}/Eu^{3+} is ^{151}Eu Mössbauer spectroscopy; these results are presented in the following section.

Of the nine crystallographically independent borate ions, only $(B8)X_3$ and $(B9)X_3$ (X = O, N) show mixed oxygen/nitrogen occupations (Table 1). Thus, approximate $BO_{1.38}N_{1.62}$ (B8) and $BO_{1.68}N_{1.32}$ (B9) moieties result. From single-crystal X-ray diffraction, no preferential distribution of trivalent and divalent europium can be derived directly. However, a closer look at bond lengths and MAPLE (Madelung part of lattice energy) calculations could elucidate this question. These considerations will be discussed below.

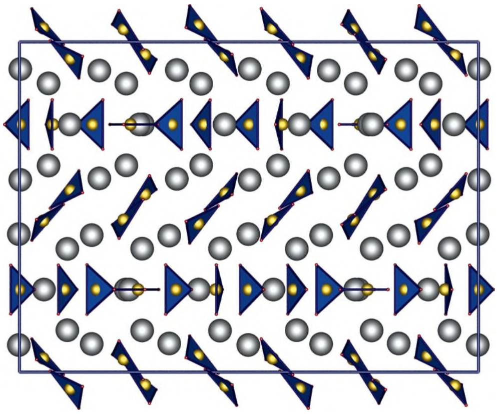

Figure 4. Crystal structure of $Eu_5(BO_{2.51(7)}N_{0.49(7)})_4$ viewed along [001]; the BX_3 moieties are shown as triangles, and light grey spheres represent the Eu atoms.

Table 1. Fractional occupation factors (f.o.f.) of the oxygen/nitrogen mixed sites in $Eu_5(BO_{2.51(7)}N_{0.49(7)})_4$.

$(B8)X_3$ (X = O, N)		$(B9)X_3$ (X = O, N)	
O81: 0.41(1)	N81: 0.59(1)	O91: 0.523(9)	N91: 0.477(9)
O82: 0.59(2)	N82: 0.41(2)	O92: 0.72(1)	N92: 0.28(1)
O83: 0.38(2)	N83: 0.62(2)	O93: 0.44(1)	N93: 0.56(1)

^{151}Eu Mössbauer Spectra of $Eu_5(BO_{2.51(7)}N_{0.49(7)})_4$

To have a sufficient amount of the Mössbauer spectroscopically active element in the specimen, a sample with the

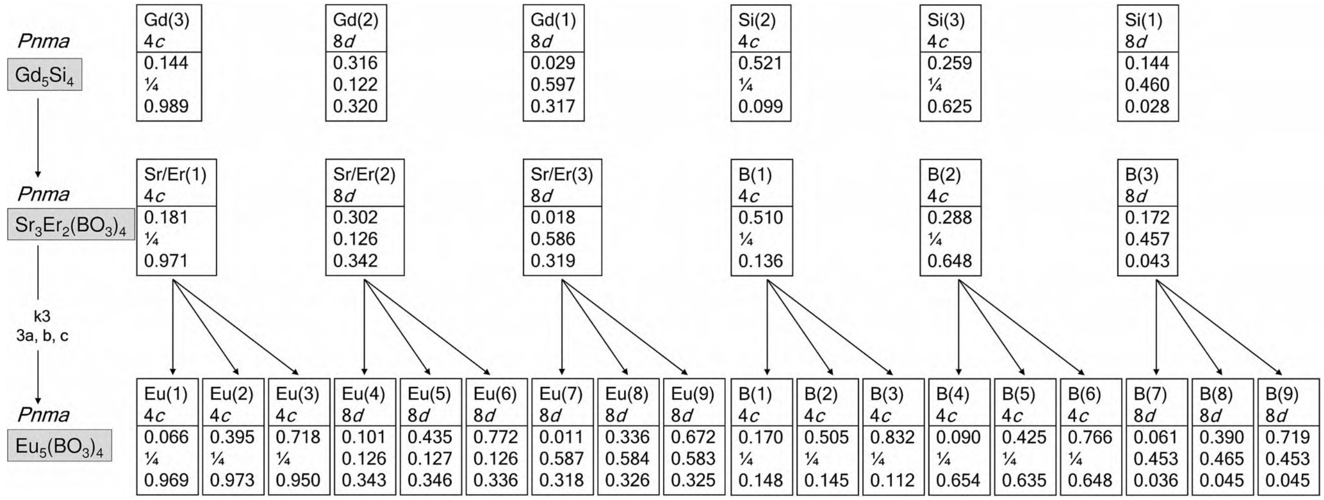

Figure 3. Group–subgroup scheme in the Bärnighausen formalism[19–22] showing the symmetry relations between Gd_5Si_4, $Sr_3Er_2(BO_3)_4$ and $Eu_5(BO_{2.51(7)}N_{0.49(7)})_4$ (only the central boron atoms of the borate ions were considered).

nominal composition $Eu_5(BO_{2.51(7)}N_{0.49(7)})_4$ was used for the ^{151}Eu Mössbauer spectroscopic investigation. The spectra recorded at 4.2, 77 and 298 K are presented in Figure 5 together with transmission integral fits. The corresponding fitting parameters are listed in Table 2. The experimental spectra could be well reproduced with a superposition of two quadrupole-split subspectra resulting from the Eu^{II} and Eu^{III} contributions. According to the intensities, approximately two thirds of the europium atoms are trivalent and one third are divalent. The isomer-shift values listed in Table 2 are close to those in binary, static mixed-valent Eu_3O_4.[23] The Eu^{II}/Eu^{III} ratio observed by Mössbauer spectroscopy is in good agreement with the electrostatic considerations based on MAPLE calculations (vide infra). The experimental line widths of the Eu^{II} and Eu^{III} signals are slightly enhanced when compared with the usually observed line width value of around 2.3 mm s^{-1}. As the structure contains several crystallographically independent europium sites, the Eu^{II} and Eu^{III} subspectra correspond to the envelope curve, as the parameters of the subspectra are very close.

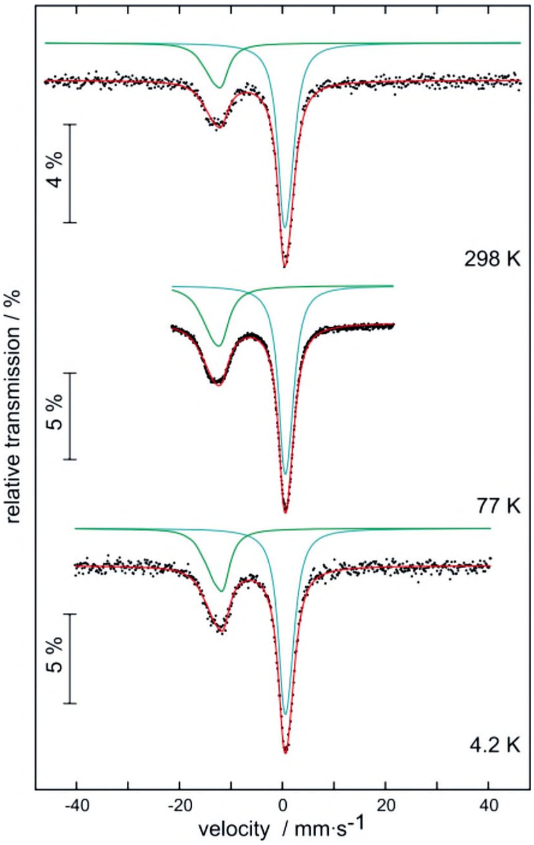

Figure 5. Experimental and simulated ^{151}Eu Mössbauer spectra of $Eu_5(BO_{2.51(7)}N_{0.49(7)})_4$ at different temperatures.

Within the estimated standard deviations of both methods, the composition $Eu_5(BO_{2.51(7)}N_{0.49(7)})_4$ obtained by the single-crystal diffraction experiment was confirmed by the Mössbauer spectroscopy results.

Table 2. Fitting parameters of the ^{151}Eu Mössbauer spectroscopic measurements of $Eu_5(BO_{2.51(7)}N_{0.49(7)})_4$ at 298, 77 and 4.2 K. The numbers in parentheses represent the statistical errors in the last digit. δ, isomer shift; Γ, experimental line width, ΔE_Q, quadrupole splitting parameter.

T /K	δ /mm s^{-1}	Γ /mm s^{-1}	ΔE_Q /mm s^{-1}	Ratio /%
298	0.71(2)	2.76(6)	–3.5(2)	75(2)
	–12.91(8)	3.4(3)	6.7(6)	25(2)
77	0.75(1)	2.68(2)	–3.22(5)	66(2)
	–13.00(2)	3.91(7)	6.8(2)	34(2)
4.2	0.77(2)	2.80(7)	–3.3(2)	68(2)
	–12.68(6)	3.31(24)	7.2(6)	32(2)

Electrostatic Considerations by Using the MAPLE Concept

For the assignment of charges to certain sites in a predominantly ionic crystal structure, lattice energy calculations based on the MAPLE concept[24,25] are an appropriate tool. All calculations on $Eu_5(BO_{2.51(7)}N_{0.49(7)})_4$, $Sr_3Er_2(BO_3)_4$ and $Sr_3Ho_2(BO_3)_4$ were performed on the basis of their refined crystal structure models. The MAPLE values differ from the sum of the MAPLE values of Eu_2O_3,[26] Er_2O_3,[27] Ho_2O_3,[28] SrO,[29] EuO,[30] EuN[31] and B_2O_3[32] within the normal ranges, that is, they are below 1 %. Our calculations confirm the partial ordering of Sr and Er/Ho in the approximate ratio 2:1 and the O/N distribution in $Eu_5(BO_{2.51(7)}N_{0.49(7)})_4$ (Tables 3, S1 and S2).

Table 3. Results of the MAPLE calculations on $Eu_5(BO_{2.51(7)}N_{0.49(7)})_4$ and average Eu–O coordination distances reduced by the ionic radius of oxide.

$Eu_5(BO_{2.51(7)}N_{0.49(7)})_4$			
MAPLE /kJ mol^{-1}	239487		
$3\Sigma_{MAPLE}(2B_2O_3 + 1.05EuO$ $+1.96EuN + 0.99Eu_2O_3)$ /kJ/mol	238838		
Δ /%	0.27		
MEFIR of Eu^{n+} /pm			
Eu1	100	Eu6	119
Eu2	121	Eu7	121
Eu3	105	Eu8	124
Eu4	110	Eu9	98
Eu5	109		
d_{avg}(Eu–O)–140 /pm			
Eu1	102	Eu6	128
Eu2	123	Eu7	126
Eu3	108	Eu8	127
Eu4	117	Eu9	99
Eu5	117		

$Eu_5(BO_{2.51(7)}N_{0.49(7)})_4$ is related to $Sr_3Ln_2(BO_3)_4$ (Ln = Er, Ho) by a threefold superstructure. In the latter compound, we observed a partial preferential occupation with strontium on sites Sr/Ln(2) and Sr/Ln(3). There are two possible reasons for this partial ordering. Either these sites are better suited electrostatically to divalent ions or, owing to their size, they are better suited to larger ions, that is, Sr^{2+} ($r_i^{CN=8}$ = 125 pm)[18] with respect to Er^{3+} ($r_i^{CN=8}$ = 100 pm);[18] it is also possible that both of these reasons are responsible for the partial ordering. In the observed threefold superstructure adopted by the mixed-valent europium compound, a complete ordering seems to be theoretically possible, especially as the ratio of the respective sites is approximately Sr/Ln = 2:1 and vice versa. Considering firstly the Eu–O coordination distances, divalent europium ions ($r_i^{CN=8}$ = 125 pm)[18] are significantly larger than trivalent europium ions ($r_i^{CN=8}$ = 107 pm).[18] Thus, for the latter, shorter coordination distances should be expected. This approach, which basically uses the coordination distances of the europium ions, was introduced by Bärnighausen[33] for $LiEu_3O_4$ and was later frequently used.[34,35]

Overall, the europium ions adopt an average positive charge of 2.79(8). Within the MAPLE calculation, Madelung effective ionic radii (MEFIR) were obtained to give us an idea of how to assign the sites to Eu^{2+} and Eu^{3+} ions in $Eu_5(BO_{2.51(7)}N_{0.49(7)})_4$ based on the size of the ions. The MEFIR values are further confirmed by the average coordination distances on all europium sites (Table 3). According to our investigation, size preferences for divalent europium are found on sites Eu2, Eu6, Eu7 and Eu8 (amounting to 28 of the 60 Eu atoms in the unit cell). The remaining sites Eu1, Eu3, Eu4, Eu5 and Eu9 might preferably host trivalent Eu ions (amounting to 32 Eu atoms).

Secondly, looking at the preferred electrostatic situation, the sites Eu1, Eu2 and Eu5 are suitable for divalent ions (Table S2) and amount to 16 europium atoms. The charges on the remaining sites are significantly larger than on these three. By also taking into account the chemical environments, these sites are to a much lower extent coordinated by nitrogen than, for example, Eu4, Eu6, Eu7, Eu8 and Eu9, which on average leads to a higher coordinating charge.

To summarise the aforementioned considerations, we conclude that from an electrostatic and crystal chemical view, the divalent ions [21(8)%] are preferentially situated on sites Eu1, Eu2 and Eu5 (27% of the europium atoms in the unit cell); this is more consistent than the assignment from the coordination distances. There, sites such as Eu6, Eu7 and Eu8, preferenced as divalent, are coordinated by a significant amount of nitridoborate moieties, and only the preference of Eu2 for divalent europium fits with the electrostatic and chemical view. A clear differentiation is difficult and cannot be derived, but the electrostatic and chemical view leads to a consistent picture of a possible Eu^{2+}/Eu^{3+} ordering.

UV/Vis Spectroscopy of $Eu_5(BO_{2.51(7)}N_{0.49(7)})_4$

The diffuse reflection spectrum of $Eu_5(BO_{2.51(7)}N_{0.49(7)})_4$ is shown in Figure 6. We observed that the reflection decreases significantly below 600 nm. The characteristic absorption of the europium ions was found in the region 370–250 nm and is attributed to Eu^{2+} 4f–5d transitions; this may also be superimposed with the charge-transfer band usually observed for trivalent europium in oxidic environments. The low-intensity narrow absorption bands are attributed to the 4f→4f transitions within trivalent europium, that is, $^7F_0 \rightarrow {}^5D_4$ (360 nm), $^7F_0 \rightarrow {}^5L_6$ (390 nm), $^7F_0 \rightarrow {}^5D_2$ (470 nm) and $^7F_0 \rightarrow {}^5D_1$ (540 nm). The measured UV/Vis absorption spectrum is in agreement with the yellow colour as well as the composition of the title compound with divalent and trivalent europium simultaneously.

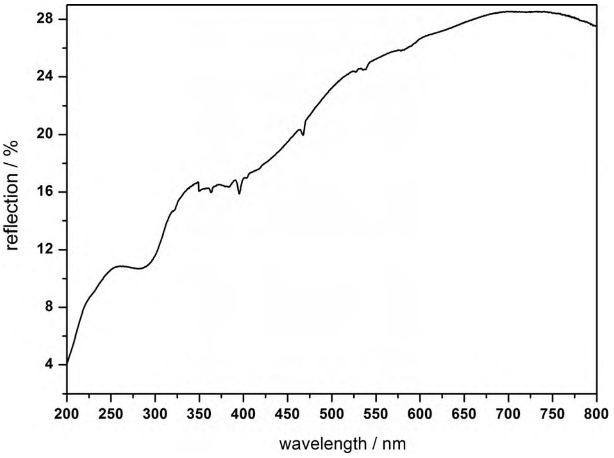

Figure 6. UV/Vis diffuse reflection spectrum of $Eu_5(BO_{2.51(7)}N_{0.49(7)})_4$.

Conclusions

In this contribution, we clarified the crystal structure of the mixed-valent borates $Sr_3Er_2(BO_3)_4$ and $Sr_3Ho_2(BO_3)_4$, which have mixed-occupancy metal-ion sites, in contrast to a previous investigation,[2] and elucidated the close relationship of the crystal structures of these borates to that of the Zintl phase Gd_5Si_4. Moreover, we then synthesised successfully the proposed europium(II,III) pendent of these borates and found a threefold superstructure of their structure type. Further investigations showed that nitrogen had been clearly incorporated to give $Eu_5(BO_{2.51(7)}N_{0.49(7)})_4$. This was proved by a careful combination of X-ray single-crystal data, ^{151}Eu Mössbauer spectroscopy and MAPLE calculations. Additionally, we could identify preferential sites for divalent europium on Eu1, Eu2 and Eu5 in $Eu_5(BO_{2.51(7)}N_{0.49(7)})_4$ on the basis of these calculations as well as crystal chemical considerations. This result is in accordance with a preferred occupation of site Sr/Er(1) with Er^{3+}, which leads to sites Eu1, Eu2 and Eu3 during the symmetry reduction, and vice versa. Finally, we were able to identify optical transitions of Eu^{2+} as well as Eu^{3+} in the reflectance spectrum, which fits with the yellow colour of $Eu_5(BO_{2.51(7)}N_{0.49(7)})_4$.

Experimental Section

Syntheses: The borates $Sr_3Er_2(BO_3)_4$ and $Sr_3Ho_2(BO_3)_4$ were synthesised according to Equation (1).

$$Ln_2O_3 + 3\,SrO + 2\,B_2O_3 \rightarrow Sr_3Ln_2(BO_3)_4 \qquad (1)$$

$Sr_3Er_2(BO_3)_4$ and $Sr_3Ho_2(BO_3)_4$: Mixtures of Er_2O_3/Ho_2O_3 (36.4/37.5 mg, 0.101 mmol, ChemPur, 99.99%), SrO (31.2 mg, 0.302 mmol, ChemPur, 99.9%) and B_2O_3 (7 mg, 1 mmol, ChemPur, 99.9%) were pulverised and transferred into boron nitride crucibles. The complete reaction was performed under a constant argon flow by applying the following temperature program: the reaction mixture was heated to 1370 K at a rate of 90 K h^{-1}, and this temperature was held for 60 h. After cooling to room temperature at a rate of 60 K/h, $Sr_3Er_2(BO_3)_4$ and $Sr_3Ho_2(BO_3)_4$ were obtained almost quantitatively as pink or yellowish nonhygroscopic crystalline powders.

$Eu_5(BO_{2.51(7)}N_{0.49(7)})_4$: The synthesis of $Eu_5(BO_{2.51(7)}N_{0.49(7)})_4$ basically follows the same procedure as that described above for $Sr_3Er_2(BO_3)_4$. In a typical synthesis, a mixture of Eu_2O_3 (87.9 mg, 0.250 mmol, ChemPur, 99.99 %) and B_2O_3 (13.9 mg, 0.200 mmol, ChemPur, 99.9 %) was pulverised and transferred into boron nitride crucibles. The complete reaction was performed by heating under a constant argon flow to 1370 K at a rate of 180 K h^{-1} and holding this temperature for 72 h. After cooling to room temperature at a rate of 90 K h^{-1}, the proposed $Eu_5(BO_3)_4$ was obtained almost quantitatively as a yellow to brownish nonhygroscopic crystalline powder. Unfortunately, the crystalline powder was well fixed to the wall of the boron nitride crucible.

The energy-dispersive X-ray spectroscopy (EDX) analysis as well as the single-crystal structure analysis gave initial evidence that the proposed $Eu_5(BO_3)_4$ contains nitrogen, which could later be proved indirectly by Mössbauer spectroscopy. Apparently, the europium oxide reacts with the boron nitride crucible and yields a partial reduction of the trivalent europium and the incorporation of nitride on oxygen sites. The exact composition was found to be $Eu_5(BO_{2.51(7)}N_{0.49(7)})_4$ from single-crystal data.

Crystal Structure Determination: Single-crystal X-ray diffraction data were collected with a Bruker AXS CCD diffractometer fitted with an APEX-II detector by using Mo-K_α radiation at room temperature and corrected for absorption by applying a multiscan correction.[36] The crystal structures of $Sr_3Er_2(BO_3)_4$, $Sr_3Ho_2(BO_3)_4$ and $Eu_5(BO_{2.51(7)}N_{0.49(7)})_4$ were solved by direct methods by using the SHELXTL program package[36] in the space group *Pnma* (no. 62) and refined with anisotropic displacement parameters for all atoms. All refinements were also performed in space group $Pna2_1$ (no. 33), in which these phases had been described before,[2] but all gave less stable refinements with significantly worse reliability factors. In the case of $Eu_5(BO_{2.51(7)}N_{0.49(7)})_4$, coupled refinements of the occupation factors of the oxygen/nitrogen sites were performed until convergence was achieved. Further single crystals of $Eu_5(BO_{2.51(7)}N_{0.49(7)})_4$ yielded the same refined O/N ratio within two estimated standard deviations (esd's). The maxima and minima of the residual electron density of the europium compound are located near the europium atoms (ca. 79 pm away); these are attributed to oscillations generated by the Fourier transform (FT) and are larger than those observed for the other compounds because of the significantly larger number of electrons per formula unit.

The compositions of the obtained samples were checked by EDX and the phase identification was performed by powder X-ray diffraction.

The relevant crystallographic data and further details of the X-ray data collection are summarised in Table 4, and selected interatomic distances and angles are listed in the Supporting Information (Table S3).

Further details on the crystal structure investigations presented in this work may be obtained from the Fachinformationszentrum Karlsruhe, Germany, 76344 Eggenstein-Leopoldshafen, Germany (fax: +49-7247-808-666; e-mail: crysdata@fiz-karlsruhe.de), on quoting the depository numbers CSD-426385 [for $Sr_3Er_2(BO_3)_4$], CSD-426386 [for $Sr_3Ho_2(BO_3)_4$] and CSD-426387 [for $Eu_5(BO_{2.51(7)}N_{0.49(7)})_4$].

Table 4. Crystal data and structure refinement.

	$Sr_3Er_2(BO_3)_4$	$Sr_3Ho_2(BO_3)_4$	$Eu_5(BO_{2.51(7)}N_{0.49(7)})_4$
Temperature /K	293(2)	293(2)	293(2)
Molar weight /g mol^{-1}	832.62	827.96	947.91
Crystal system	orthorhombic	orthorhombic	orthorhombic
Space group	*Pnma*	*Pnma*	*Pnma*
Crystal shape	block	block	plate
Colour	light pink	pink	yellow
a /Å	7.3808(2)	7.3845(7)	22.322(5)
b /Å	15.8894(4)	15.9155(12)	16.031(3)
c /Å	8.6781(2)	8.7103(9)	8.7959(18)
V /Å^3	1017.74(4)	1023.70(16)	3147.5(11)
Z	4	4	12
Calculated density ρ_x /g cm^{-3}	5.43	5.37	6.28
μ /mm^{-1}	32.0	30.9	29.5
F(000)	1464	1456	5154
Radiation (λ /Å)	Mo-K_α (0.71073)	Mo-K_α (0.71073)	Mo-K_α (0.71073)
Absorption correction	multiscan	multiscan	multiscan
Max. *h*/*k*/*l*	7/17/9	7/17/9	28/20/11
θ range /°	2.56–22.50	2.56–22.50	3.13–27.45
Measured reflections	5072	5975	70505
Independent reflections	683	691	3719
Observed reflections	597	513	3352
Parameters refined	70	59	317
R_{int}, R_σ	0.045, 0.024	0.134, 0.072	0.049, 0.021
R_1 (all data)	0.037	0.069	0.027
wR_2 (all data)	0.077	0.098	0.059
GooF	1.073	0.989	1.026
Residual electron density, min./max.	–0.84/2.28	–1.37/2.28	–3.34/3.18

X-ray Powder Diffractometry: The crystalline samples were enclosed in glass capillaries with a diameter of 0.2 mm and investigated at room temperature in Debye–Scherrer geometry with a STOE Stadi P powder diffractometer with Ge(111)-monochromatised Mo-K_α radiation (linear PSD detector, step width 0.5°, acquisition time: 90 s/step). The obtained crystalline products $Sr_3Er_2(BO_3)_4$ and $Sr_3Ho_2(BO_3)_4$ were phase pure according to X-ray powder diffractometry, whereas in the powder pattern of $Eu_5(BO_{2.51(7)}N_{0.49(7)})_4$, weak BN reflections owing to adhesive crucible traces could be identified as a single contaminant (Figure 7).

^{151}Eu Mössbauer Spectroscopy: The 21.53 keV transition of ^{151}Eu with an activity of 130 MBq (2% of the total activity of a ^{151}Sm:EuF$_3$ source) was used for the Mössbauer spectroscopic experiments, which were conducted in the usual transmission geometry. The measurements were performed with a commercial helium-bath cryostat. The temperature of the absorber was varied between 4.2 K and room temperature, and the source was kept at room temperature. The temperature was controlled by a resistance thermometer (±0.5 K accuracy). The sample of $Eu_5(BO_{2.51(7)}N_{0.49(7)})_4$ was enclosed in a small PVC container at a thickness corresponding to ca. 10 mg of Eu/cm^2.

Supporting Information (see footnote on the first page of this article): Tables of the MAPLE calculations on the title compounds.

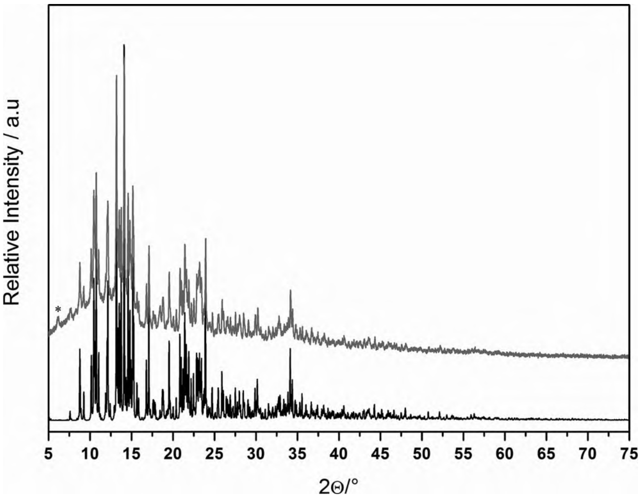

Figure 7. Comparison of a measured diffraction pattern of $Eu_5(BO_{2.51(7)}N_{0.49(7)})_4$ (above) and a calculated powder diffraction pattern on the basis of our structure model (below), a reflection of hexagonal BN is marked (*).

Acknowledgments

The authors thank Michel U. Panzer (Albert-Ludwigs-Universität Freiburg) for his work as a project student. This work was financially supported by the Deutsche Forschungsgemeinschaft (DFG) (to R. P. and I. S.).

---

[1] W. Yen, S. Shionoya, H. Yamamoto, *Phosphor Handbook*, CRC Press/Taylor and Francis, **2007**.

[2] G. K. Abdullaev, C. Mamedov, *Zh. Strukt. Khim.* **1976**, *17*, 188.

[3] R. Mueller-Mach, G. Mueller, M. R. Krames, H. A. Höppe, F. Stadler, W. Schnick, T. Jüstel, P. Schmidt, *Phys. Status Solidi A* **2005**, *202*, 1727.

[4] C. Ronda, *J. Lumin.* **2002**, *100*, 301.

[5] V. K. Il'in, B. F. Dzhurinskii, V. M. Novotortsev, I. V. Tananaev, *Izv. Akad. Nauk SSSR Neorg. Mater.* **1980**, *16*, 1304–1305.

[6] K. Machida, H. Hata, K. Okuno, G. Adachi, J. Shiokawa, *J. Inorg. Nucl. Chem.* **1979**, *41*, 1425.

[7] K. Machida, G. Adachi, J. Shiokawa, *Acta Crystallogr., Sect. B* **1980**, *36*, 2008.

[8] K. Machida, G. Adachi, J. Shiokawa, *Acta Crystallogr., Sect. B* **1979**, *35*, 149.

[9] A. Goriounova, P. Held, P. Becker, L. Bohatý, *Acta Crystallogr., Sect. E* **2004**, *60*, i131.

[10] H. Emme, H. Huppertz, *Chem. Eur. J.* **2003**, *9*, 3623.

[11] M. Orth, W. Schnick, *Z. Anorg. Allg. Chem.* **1999**, *625*, 551–554.

[12] O. Reckeweg, H.-J. Meyer, *Z. Anorg. Allg. Chem.* **1999**, *625*, 866–874.

[13] W. Carrillo-Cabrera, M. Somer, K. Peters, H.-G. von Schnering, *Z. Kristallogr. New Cryst. Struct.* **2001**, *216*, 43–44.

[14] S. Schmid, W. Schnick, *Z. Anorg. Allg. Chem.* **2002**, *628*, 1192–1195.

[15] H. A. Höppe, S. J. Sedlmaier, *Inorg. Chem.* **2007**, *46*, 3467.

[16] H. A. Höppe, *J. Solid State Chem.* **2009**, *182*, 1786–1791.

[17] S. Misra, G. J. Miller, *J. Am. Chem. Soc.* **2008**, *130*, 13900.

[18] D. Shannon, C. T. Prewitt, *Acta Crystallogr., Sect. B* **1969**, *25*, 925.

[19] H. Bärnighausen, *Commun. Math. Chem.* **1980**, *9*, 139.

[20] U. Müller, *Z. Anorg. Allg. Chem.* **2004**, *630*, 1519.

[21] U. Müller, in: *International Tables for Crystallography*, vol. A1, *Symmetry relations between space groups* (Eds.: H. Wondratschek, U. Müller), 2nd ed., John Wiley & Sons Ltd., Chichester, UK, **2010**, p. 44–56.

[22] U. Müller, *Symmetriebeziehungen zwischen verwandten Kristallstrukturen*, Vieweg + Teubner, Wiesbaden, Germany, **2012**.

[23] H. H. Wickman, E. Catalano, *J. Appl. Phys.* **1968**, *39*, 1248–1249.

[24] a) R. Hoppe, *Angew. Chem.* **1966**, *78*, 52; *Angew. Chem. Int. Ed. Engl.* **1966**, *5*, 95; b) R. Hoppe, *Angew. Chem.* **1970**, *82*, 7; *Angew. Chem. Int. Ed. Engl.* **1970**, *9*, 25.

[25] R. Hübenthal, *MAPLE, Program for the Calculation of the Madelung Part of Lattice Energy*, **1993**.

[26] R. C. Rau, *Proc. Conf. Rare Earth Res. (3rd)* **1963**, 1964.

[27] A. Fert, *Acta Crystallogr., Sect. B* **1984**, *40*, 76.

[28] W. C. Koehler, E. O. Wollan, M. Wilkinson, *Phys. Rev.* **1958**, *110*, 37.

[29] W. Primak, H. Kaufman, R. Ward, *J. Am. Chem. Soc.* **1948**, *70*, 2043.

[30] H. A. Eick, N. C. Baenziger, L. Eyring, *J. Am. Chem. Soc.* **1956**, *78*, 5147.

[31] H. Jacobs, U. Fink, *Z. Anorg. Allg. Chem.* **1978**, *438*, 151.

[32] G. E. Gurr, P. W. Montgomery, C. D. Knutson, B. T. Gorres, *Acta Crystallogr., Sect. B* **1970**, *26*, 906.

[33] H. Bärnighausen, *Z. Anorg. Allg. Chem.* **1970**, *374*, 201.

[34] S. Hammerich, I. Pantenburg, G. Meyer, *Z. Anorg. Allg. Chem.* **2006**, *632*, 1487.

[35] C. Wickleder, *Z. Anorg. Allg. Chem.* **2002**, *628*, 1815.

[36] a) *SADABS: Area-Detector Absorption Correction*; Siemens Industrial Automation Inc., Madison, **1996**; b) G. M. Sheldrick, *SHELXTL*, v. 5.10, *Crystallographic System*, Bruker AXS Analytical X-ray Instruments Inc., Madison, **1997**.